Short-term effect of 1% atropine on the thickness of the ciliary muscle in children

Zhao-Yu Xiang[1,2], Li-Pu Cui[1,2], Chun Tang[1], Hai-Dong Zou[1,2*] and Yan Xu[1*]

[1] Department of Ophthalmology, Shanghai Eye Diseases Prevention & Treatment Center/Shanghai Eye Hospital, School of Medicine, Tongji University, Shanghai 200331, China

[2] Department of Ophthalmology, Shanghai Clinical Research Center for Eye Diseases, Shanghai Key Clinical Specialty, Shanghai Key Laboratory of Ocular Fundus Diseases, Shanghai Engineering Center for Visual Science and Photomedicine, Shanghai Engineering Center for Precise Diagnosis and Treatment of Eye Diseases, National Clinical Research Center for Eye Diseases, Shanghai General Hospital/Shanghai Jiao Tong University School of Medicine, Shanghai 200080, China

* Corresponding authors, E-mail: zouhaidong@sjtu.edu.cn; drxuyan_2004@163.com

Abstract

The impact of atropine on the ciliary muscle and its correlation with the choroid remain unclear. This study aimed to investigate changes in the ciliary muscle before and after atropine treatment and its influencing factors. Children (3–12 years; 12 with myopia, 17 with emmetropia, and 19 with hyperopia) received 1% atropine for 1 week. Optometry and ocular biometry were performed before and after treatment, focusing on changes in the ciliary muscle. Nasal ciliary parameters from 48 right eyes were analyzed. Paired t-tests assessed cycloplegia-induced changes; one-way analysis of variance compared refractive groups. Pearson correlations and stepwise multiple linear regression evaluated associations and confounders. The Benjamini–Hochberg correction was applied for multiple comparisons. At baseline, posterior ciliary muscle thickness correlated positively with axial length ($r = 0.538$, $p = 0.0023$) and negatively with choroidal thickness ($r = -0.396$, $p = 0.032$). After atropine treatment, the ciliary muscles thickened with posterior displacement, particularly posteriorly (myopia: 56.20 ± 40.10 μm; emmetropia: 104.49 ± 77.94 μm; hyperopia: 138.36 ± 88.33 μm; all $p < 0.001$). Thicker baseline ciliary muscle was associated with less thickening (all $p < 0.01$). Baseline posterior ciliary muscle thickness increased with axial length and decreased with choroidal thickness; axial length mediated the choroid–ciliary muscle association, supporting the choroidal stretching hypothesis. Atropine increased the spherical equivalent in all groups. Contrary to the expected thinning, ciliary muscle thickened after treatment, indicating effects beyond cycloplegia.

Introduction

Atropine, a muscarinic antagonist, is used in visual examinations, for treating amblyopia, and for controlling myopia[1,2]. Atropine is important in pediatric ophthalmology as a powerful cycloplegic agent and myopia treatment. Compared with adults, children have a greater maximum accommodative amplitude and a more pronounced accommodative lag[3]. Accommodation plays an important role in children's refractive development and is closely related to refractive errors. Near-distance work is a significant risk factor for myopia[4–6]. Myopic eyes have been reported to take a longer time to recover from the axial elongation caused by accommodation than emmetropic eyes[7].

During accommodation, the ciliary muscle contracts, which is associated with myopic drift. In the 20th century, studies have observed the forward movement of the ciliary muscle during accommodation in histological sections[8–11] and via goniovideography[12–14]. Subsequently, the use of ultrasound biomicroscopes (UBMs) has enabled direct visualization of the forward movement of the ciliary muscle[15,16] and revealed the thickening of the anterior segment of the ciliary muscle during accommodation[16–18]. Currently, the high resolution of anterior segment optical coherence tomography (AS-OCT) facilitates more precise observation. Studies using AS-OCT revealed that the posterior area of the ciliary muscle thinned during accommodation[17–23].

Ciliary muscle thickness (CMT) differs in individuals with different refractive errors. Several studies have found that the ciliary muscle became thicker with an increase in axial length (AL)[21,24–26]. Some studies have suggested that myopia primarily affects the posterior area of the ciliary muscle[19,24,27–30]. However, hyperopic anterior

segment morphology and myopic posterior remodeling remain mechanistically contested[25,28,30,31].

While atropine's dual functions as a cycloplegic agent and a myopia control intervention are widely recognized[32,33], and its choroidal thickening effect is documented[33–36], recent studies indicate diminished effects in hyperopic children[37]. Importantly, morphological changes in the ciliary muscle after atropine administration remain incompletely characterized. Furthermore, potential relationships between the ciliary muscle and choroidal responses have not been clearly examined. This study employed AS-OCT to characterize morphological alterations in the ciliary muscle after 1% atropine treatment. We aimed to document responses across refractive groups, identify factors influencing baseline ciliary parameters and their changes, and provide clinical evidence elucidating atropine's mechanisms of action.

Materials and methods

Study participants and atropine treatment

Children aged 3–12 years who visited the Shanghai Eye Disease Prevention and Control Center, China, between December 2020 and April 2021 were enrolled. The exclusion criteria included the following: (1) allergy to atropine; (2) eye diseases other than refractive errors; (3) any previous correction or treatment of refractive error (including corrective lenses); (4) a history of ocular trauma or ocular surgery; (5) systemic disease; and (6) patients who were unable to cooperate with the inspection. The study was conducted in accordance with the Declaration of Helsinki. The study protocol was approved by the Ethics Committee of Shanghai General Hospital,

Shanghai Jiao Tong University (2020KY018), and written informed consent was obtained from the participants and their parents.

Forty-nine children aged 3–12 years (7.10 ± 1.49 years) were screened, and 48 were enrolled (27 boys, 21 girls); one child was excluded due to loss to follow-up. Each patient visit was assigned a unique 10-digit code unrelated to identifiable information. All examinations and image measurements were performed by technicians masked to the study protocol. Technicians could only access the patients' code and were unaware of the other examination results.

Parents administered one drop of 1% atropine to each eye of their child every night for 7 consecutive days. Before the treatment's initiation, ophthalmologists provided onsite instruction to the parents and supplied instructional videos on proper atropine administration. Treatment commenced the day following the baseline visit, and patients returned for re-examination the day after completing the treatment course. Following the post-treatment examination, ophthalmologists diagnosed and managed patients on the basis of the findings. Adverse events were recorded for each child during the study visit. All adverse events, regardless of their suspected relationship to atropine use, were documented.

Examination

Each participant underwent a series of ophthalmic examinations before and after atropine-induced cycloplegia. Refractive measurements were obtained without cycloplegia at baseline and under cycloplegia after atropine treatment. Objective refraction was measured using an autorefractor (KR-8800, Topcon, Japan). Subjective refinement was then conducted using a phoropter (RT-3100, Nidek, Japan) to determine the spherical equivalent (SE = sphere + 1/2 cylinder). Best-corrected visual acuity (BCVA) was assessed at 5 m and recorded in logMAR. AL and anterior chamber depth (ACD) were measured using an IOLMaster 700 (Carl Zeiss Meditec, Dublin, CA, USA), with the average of six measurements recorded. Intraocular pressure was measured using a non-contact tonometer (NT-510, Nidek, Japan), and the average of three measurements was recorded. Atropine was not administered if the intraocular pressure exceeded 21 mmHg.

Choroidal thickness (CT) measurement

CT was measured using swept-source optical coherence tomography (DRI OCT-1 Atlantis, Topcon, Japan). Layer segmentation was performed automatically using built-in software, with manual correction applied when the software incorrectly identified layer boundaries. The Early Treatment Diabetic Retinopathy Study grid within the built-in software was used to calculate the average CT within each grid sector. The diameters of the subfoveal, parafoveal, and perifoveal circles were 1, 3, and 6 mm, respectively. CT was measured in the subfoveal region and the parafoveal region (calculated as the average of the four quadrants; Fig. 1).

Ciliary muscle imaging and measurement

Ciliary muscle imaging was performed using AS-OCT (SS-1000, Tomey, Japan). An external fixation target was used during imaging. The fixation point was positioned using a goniometer at 55° and 30 cm from the device's central axis, with the patient's chin and head stabilized at 0° (parallel to the AS-OCT axis). Images of the ciliary muscle were acquired in the temporal, inferior, nasal, and superior quadrants by having the patient fixate in the opposite direction. Images with poorly defined ciliary muscle boundaries were reacquired. If satisfactory image quality could not be achieved after three consecutive attempts, the image was recorded as missing. Due to poor image quality, inferior and superior quadrant images were excluded from subsequent measurements. A suitable imaging plane was then selected by the technician using the built-in software (Fig. 2). A suitable plane was defined as one where the scan line passed through the pupil's center. A refractive index of 1.000 was applied to the entire image.

Ciliary muscle parameters for each quadrant were averaged from three images. Measurements were performed using AutoCAD 2014 software. First, the exported image's built-in scale bar was used for calibration to millimeters (Fig. 3a). Second, the 'curve fitting' tool was used to manually trace the contour of the ciliary muscle (Fig. 3b). Third, perpendicular lines were drawn perpendicular to the scleral curvature at two points (the scleral spur and the point of maximum ciliary muscle thickness). The distance from the thickest point to the inner scleral border defined the maximum ciliary muscle thickness (CMTmax) (Fig. 3c, d). Subsequently, the 'Array-path' function was used to generate additional perpendicular lines spaced at 1-mm intervals along the scleral curvature, starting from the scleral spur (Fig. 3c). The distance between the intersection points of each perpendicular line with the inner and outer ciliary muscle boundaries was measured as the CMT at that location (Fig. 3d). The ciliary muscle's thickness at 1, 2, and 3 mm from the scleral spur was termed CMT1, CMT2, and CMT3, respectively
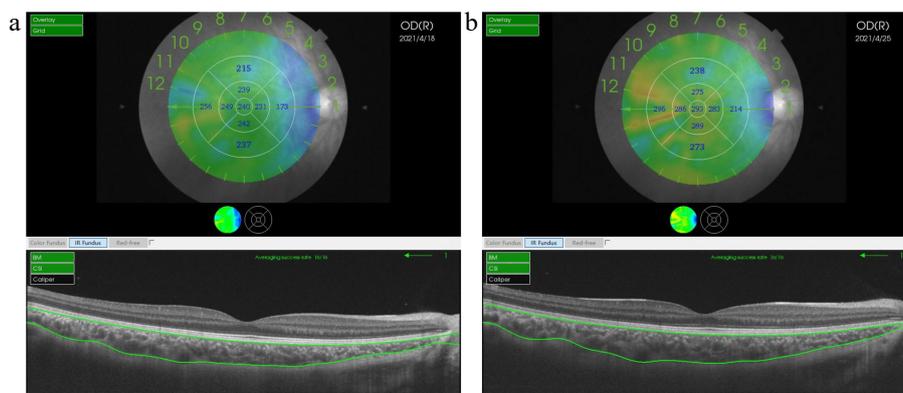

Fig. 1 Choroidal thickness measurements using swept-source optical coherence tomography. (a) Baseline choroidal imaging. (b) Post-atropine choroidal imaging. Representative images show a cross-sectional B-scan (below) with automated choroidal segmentation (green outline) and an en-face view (above) with the Early Treatment Diabetic Retinopathy Study (ETDRS) grid overlay. The en-face map includes an orientation scale (1–12) corresponding to the B-scan positions. Arrows indicate Orientation 1, corresponding to the B-scan displayed below. Subfoveal choroidal thickness was measured vertically at the foveal center. Parafoveal choroidal thickness was calculated as the average of measurements in the four quadrants of the 3-mm diameter ETDRS ring. A color-coded thickness map on the ETDRS grid shows the distribution of choroidal thicknesses (warmer colors indicate thicker areas).
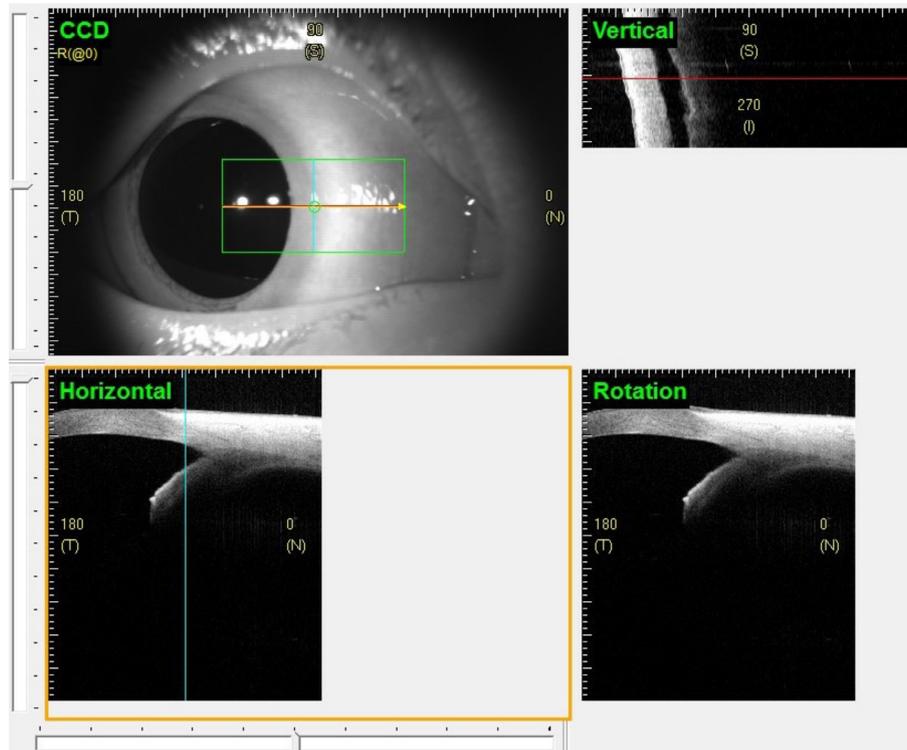
Page 2 of 9

Xiang et al. Visual Neuroscience 2025, 42: e022

Fig. 2 Imaging plane selection protocol for measuring ciliary muscles using anterior segment OCT (AS-OCT). Upper left: External view showing eye positioning with the fixation target at 55° and 30 cm from the central axis of the device, while maintaining the chin and head at 0°. The green selection box indicates the AS-OCT scan area. There are three lines in the green selection box; the cyan vertical line can move horizontally, and the red horizontal line can move vertically. The yellow rotation line can be rotated around the intersection of the horizontal and vertical lines. A suitable plane can be selected by adjusting the lines' positions. In this image, the rotation line is hidden behind the horizontal line (the rotation angle is 0°). Upper right: Vertical cross-section corresponding to the cyan line's position. Lower left: Horizontal cross-section corresponding to the red line's position. Lower right: Rotational cross-section corresponding to the yellow rotation line's position.

(Fig. 3d). A tangent line was drawn along the pigmented ciliary muscle epithelium (the posterior ciliary boundary), originating from the scleral spur. A perpendicular line was then dropped from the thickest point to this tangent line (Fig. 3e). The distance along the tangent line from the scleral spur to the foot of this perpendicular defined the position parameter of the ciliary muscle's apex (CMAL) (Fig. 3f).

Statistical analysis

The Kolmogorov–Smirnov test was used to assess normality for all variables. Normally distributed data are presented as the mean ± standard deviation, and non-normally distributed descriptive data are presented as medians (Quartile 1, Quartile 3). Because of significant interocular correlation ($p < 0.05$), data from the right eye were used for analysis. The parameters of the temporal and nasal ciliary muscles were significantly correlated ($p < 0.05$). Therefore, nasal ciliary muscle parameters were analyzed.

Paired t-tests were used for normally distributed data, and Wilcoxon's signed-rank tests were used for non-normally distributed data to assess changes before and after cycloplegia. One-way analysis of variance was used to compare groups for normally distributed data, with Bonferroni correction applied for post hoc pairwise comparisons. The Kruskal–Wallis test was used for non-normally distributed data to compare groups. Pearson's correlation coefficient was calculated to assess associations between normally distributed parameters. Multiple linear regression models were used to adjust for potential confounding factors. Stepwise multiple linear regression was used to analyze factors influencing changes in the ciliary muscle's biometry after cycloplegia. Sex was coded as male =

1 and female = 0. Variables were entered into the model if $p \le 0.05$ and removed if $p \ge 0.10$.

The Benjamini–Hochberg procedure was used to control the false discovery rate for multiple comparisons. Statistical significance was defined as $p < 0.05$ after correction. Statistical analyses were performed using SPSS software (version 22, International Business Machines Corporation, USA).

Results

Participants

Participants were categorized into three groups depending on the SE after cycloplegia: myopia: SE < −0.5 D, $n = 12$; emmetropia: −0.5 $D \le$ SE ≤ 0.5 D, $n = 17$; hyperopia: SE > 0.5 D, $n = 19$. There was no significant difference in age among the groups ($F = 1.54$, $p = 0.23$).

Spherical equivalent, axial length, and anterior chamber depth

Significant between-group differences were observed at baseline for SE ($H = 32.35$, $p < 0.001$), AL ($F = 17.32$, $p < 0.001$), and ACD ($F = 14.13$, $p < 0.001$). The hyperopia group had a significantly shorter AL and shallower ACD compared with both the myopia and emmetropia groups (all $p < 0.001$). After atropine treatment, SE increased (myopia: $p = 0.002$; emmetropia and hyperopia: $p < 0.001$), AL decreased (all $p < 0.001$), and ACD increased (all $p < 0.001$) in all groups. However, the magnitude of the change in ACD was significantly greater in the hyperopia group compared with both the myopia and emmetropia groups (both $p < 0.001$; Table 1).
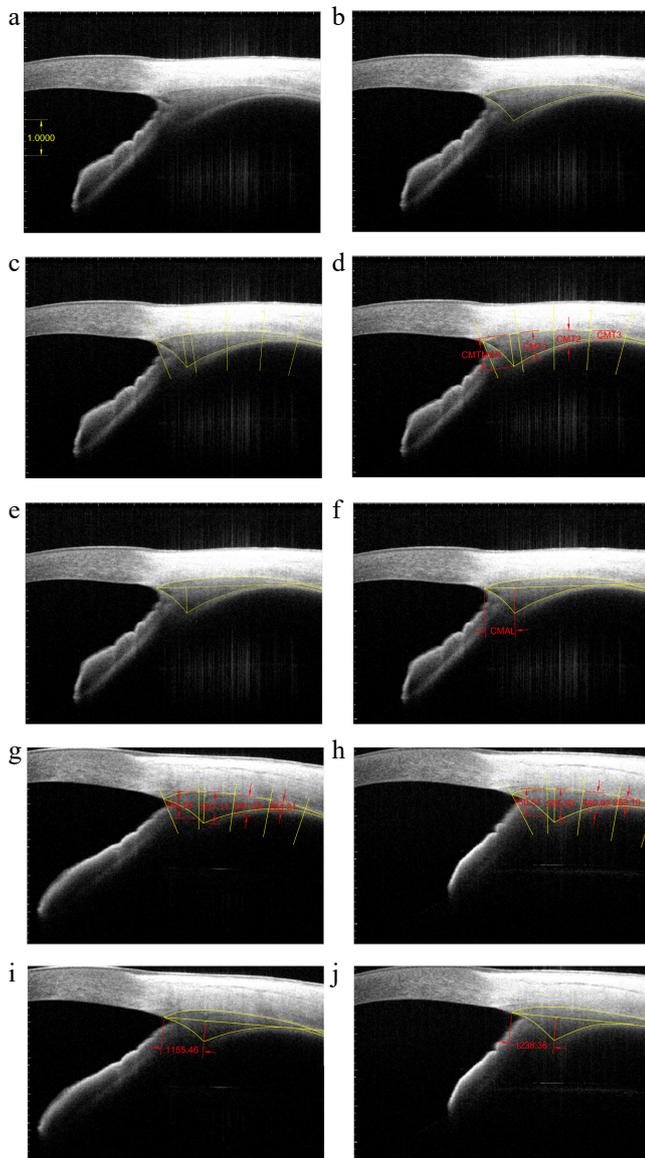
Fig. 3 Measurement of ciliary muscle parameters using anterior segment optical coherence tomography. (a) An internal 1-mm ruler was used for calibration (white scale bar). (b) Contouring: Manual tracing of the ciliary muscle's contour (yellow curves). (c) Thickness landmark placement: Placement of perpendicular measurement lines (yellow straight lines) at 1-mm intervals along the scleral curvature (outer ciliary muscle boundary) from the scleral spur. (d) Thickness parameters (red double arrows and red labels): Ciliary muscle thickness at 1 (CMT1), 2 (CMT2), and 3 mm (CMT3) posterior to the scleral spur (SS), and maximum thickness (CMTmax). (e) Position landmark placement: Placement of a tangent line (yellow horizontal line) along the pigmented ciliary muscle epithelium (the posterior ciliary muscle boundary). (f) Position parameter (red double arrows and red label): Distance along tangent line from the scleral spur to the foot of the perpendicular from CMTmax point was regarded as the CMAL. (g) Baseline thickness parameters (red text). (h) Thickness parameters after atropine treatment (red text). (i) Baseline position parameters (red text). (j) Position parameters after atropine treatment (red text).

Choroidal thickness

At baseline, significant between-group differences were observed for subfoveal CT (F = 7.24, p = 0.002) and parafoveal CT (F = 7.03, p = 0.002). Subfoveal and parafoveal CT were significantly thicker in the hyperopia group compared with the myopia group (subfoveal: p =

0.018; parafoveal: p = 0.011) and the emmetropia group (subfoveal: p = 0.003, parafoveal: p = 0.006; Table 1).

In the myopia group, subfoveal CT (p = 0.026) and parafoveal CT (p < 0.001) increased significantly after atropine treatment. In the emmetropia group, only subfoveal CT increased significantly (p = 0.012); the change in parafoveal CT was not significant (p = 0.054). In the hyperopia group, neither subfoveal CT (p = 0.986) nor parafoveal CT (p = 0.763) changed significantly after treatment (Table 1).

Ciliary muscle biometry

At baseline, significant between-group differences were found for CMT2 (F = 5.48, p = 0.008) and CMT3 (F = 5.54, p = 0.007), but not for CMT1, CMTmax, or CMAL (all p > 0.05; Table 2). Both CMT2 and CMT3 were significantly thinner in the hyperopia group compared with the myopia group (CMT2: p = 0.026; CMT3: p = 0.026) and the emmetropia group (CMT2: p = 0.02; CMT3: p = 0.018; Table 2).

After atropine treatment, CMT2 (all p < 0.001) and CMT3 (myopia group: p = 0.001; emmetropia and hyperopia groups: p < 0.001) increased significantly in all groups (Fig. 3g, h). CMAL increased significantly in all groups (myopia group: p = 0.017; emmetropia group: p < 0.001; hyperopia group: p = 0.009; Fig. 3i, j). CMT1 (myopia group: p = 0.105; emmetropia and hyperopia groups: p < 0.001) and CMTmax (myopia group: p = 0.157; emmetropia and hyperopia groups: p < 0.001) increased significantly in the emmetropia and hyperopia groups but not in the myopia group (Table 2).

Factors influencing baseline ciliary muscle parameters

Correlation analysis revealed no significant association between age and baseline ciliary parameters (all p > 0.05; Fig. 4). No statistically significant differences in any ciliary muscle parameters (CMT1, CMT2, CMT3, CMTmax, and CMAL) were found between the sexes (all p > 0.05). AL was positively correlated with CMT2 (r = 0.538, p = 0.0023) and CMT3 (r = 0.491, p = 0.0082). No significant correlations were observed between AL and CMT1, CMTmax, or CMAL (all p > 0.05; Fig. 4). CT values exhibited negative correlations with CMT2 (subfoveal CT: r = −0.396, p = 0.032; parafoveal CT: r = −0.409, p = 0.032). CMT1, CMT3, CMTmax, and CMAL showed no significant correlations with CT values (all p > 0.05; Fig. 4).

Multiple linear regression analysis was performed using different ciliary muscle parameters as the dependent variables and age, sex, AL, subfoveal CT, and parafoveal CT as the independent variables. This revealed that CMT1, CMTmax, and CMAL had no significant associations with any independent variables (all p > 0.05). After multivariate adjustment, CMT2 (standardized β = 0.619, p = 0.001) and CMT3 (standardized β = 0.599, p = 0.003) were positively correlated only with AL. Age, sex, subfoveal CT, and parafoveal CT showed no significant associations (all p > 0.05) in these models.

Univariate regression demonstrated negative correlations between subfoveal CT and CMT2, and between parafoveal CT and CMT2 (consistent with the correlation analysis results). In univariate analyses, AL was negatively correlated with both subfoveal CT (standardized β = −0.551, p < 0.001) and parafoveal CT (standardized β = −0.512, p < 0.001). However, when AL was included in the regression models of CT (subfoveal or parafoveal) and CMT2, the regression coefficients for CT became nonsignificant (subfoveal CT: standardized β = −0.134, p = 0.391; parafoveal CT: standardized β = −0.172, p = 0.256).

Factors affecting changes in ciliary muscle parameters after atropine treatment

Stepwise multiple linear regression analysis revealed that changes in CMT parameters (CMT1, CMT2, CMT3, CMTmax; Supplementary Fig. S1a–d) and CMAL were negatively correlated with their

Table 1. Anterior segment biometry before and after 1% atropine treatment in myopic, emmetropic, and hyperopic children.

	Myopia (n = 12)		Emmetropia (n = 17)		Hyperopia (n = 19)	
	Baseline	Difference	Baseline	Difference	Baseline	Difference
Age (mean ± SD, years)[c]	6.76 ± 1.25		7.60 ± 1.53		6.86 ± 1.55	
SE (median (Q1, Q3), D)[d]	−2.13 (−3.19, −1.50)[a]	0.88 (0.50, 1.00)[b]	−0.75 (−0.88, −0.50)[a]	0.75 (0.50, 1.00)[b]	1.88 (0.19, 3.50)	1.13 (1.75, 2.50)[b]
AL (mean ± SD, mm)[c]	23.74 ± 0.93[a]	−0.03 ± 0.02[b]	23.49 ± 0.89[a]	−0.02 ± 0.02[b]	21.87 ± 1.12	−0.03 ± 0.03[b]
ACD (mean ± SD, mm)[c]	3.72 ± 0.28[a]	0.10 ± 0.04[b]	3.65 ± 0.23[a]	0.13 ± 0.07[b]	3.29 ± 0.23	0.30 ± 0.15[b]
Subfoveal CT (mean ± SD, μm)[c]	244.33 ± 34.46[a]	29.67 ± 40.08[b]	240.29 ± 44.28[a]	18.06 ± 26.28[b]	291.00 ± 48.11	0.16 ± 38.98
Parafoveal CT (mean ± SD, μm)[c]	239.00 ± 32.98[a]	21.73 ± 13.47[b]	241.18 ± 38.92[a]	10.74 ± 21.33	283.95 ± 42.63	2.55 ± 36.40

Table 1 lists the basic information and anterior segment biometry of the three groups. 'Baseline' refers to the parameters before atropine-induced cycloplegia, and 'Difference' represents the change in each parameter after cycloplegia compared with before treatment (positive values indicate an increase, negative values indicate a decrease). SE, spherical equivalent; Q1, Quartile 1; Q3, Quartile 3; AL, axial length; SD, standard deviation; ACD, anterior chamber depth; CT, choroidal thickness. [a] Significantly different compared with the hyperopic group at baseline, $p < 0.05$. [b] Significantly changed after atropine, $p < 0.05$. [c] Normally distributed data represented by the mean ± SD; the paired t-test was used to test the differences before and after cycloplegia. [d] Skewed distribution data represented by the median (Q1, Q3); the Wilcoxon test was used to test the differences before and after cycloplegia.

Table 2. Ciliary muscle parameters before and after 1% atropine treatment in myopic, emmetropic, and hyperopic children.

	Myopia		Emmetropia		Hyperopia	
	Baseline	Difference	Baseline	Difference	Baseline	Difference
CMT1 (mean ± SD, μm)	728.62 ± 130.93	59.58 ± 116.77	755.50 ± 126.36	133.95 ± 101.59[b]	751.98 ± 89.74	135.91 ± 88.05[b]
CMT2 (mean ± SD, μm)	444.06 ± 91.77[a]	56.20 ± 40.10[b]	435.61 ± 104.38[a]	104.49 ± 77.94[b]	343.65 ± 88.57	138.36 ± 88.33[b]
CMT3 (mean ± SD, μm)	190.51 ± 56.88[a]	49.60 ± 38.98[b]	187.95 ± 51.16[a]	64.79 ± 61.20[b]	134.45 ± 49.24	97.29 ± 53.91[b]
CMTmax (mean ± SD, μm)	864.15 ± 84.00	36.73 ± 83.70	838.81 ± 106.84	133.95 ± 90.34[b]	845.48 ± 110.74	112.45 ± 71.82[b]
CMAL (mean ± SD, μm)	822.50 ± 181,62	131.67 ± 162.47[b]	774.71 ± 153.59	215.88 ± 180.70[b]	750.59 ± 117.13	102.35 ± 140.91[b]

Table 2 lists ciliary muscle parameters at baseline and after the atropine intervention in myopic, emmetropic, and hyperopic groups. 'Baseline' refers to the parameters before atropine-induced cycloplegia, and 'Difference' represents the change in each parameter after cycloplegia compared with before the treatment (positive values indicate an increase; negative values indicate a decrease). Ciliary muscle parameters are represented by the mean ± SD, and the paired t-test was used to test the differences before and after cycloplegia. CMT1, ciliary muscle thickness at 1 mm from the scleral spur; SD, standard deviation; CMT2, ciliary muscle thickness at 2 mm from the scleral spur; CMT3, ciliary muscle thickness at 3 mm from the scleral spur; CMTmax, maximum ciliary muscle thickness; CMAL, tangent length from the ciliary muscle apex to the scleral spur. [a] Significantly different compared with the hyperopic group at baseline, $p < 0.05$. [b] Significantly changed after atropine, $p < 0.05$.

respective baseline values (Supplementary Fig. S1e). Baseline SE was positively correlated with the change in CMT1 (Supplementary Fig. S1f) and negatively correlated with the change in CMAL (Supplementary Fig. S1g) after atropine treatment (both $p < 0.05$). Sex, age, subfoveal CT, and parafoveal CT were not significant predictors in the final models (all $p > 0.05$; see the Supplementary file 1 for detailed regression models).

Discussion

In this study, children were categorized into myopia, emmetropia, and hyperopia groups. After atropine treatment, all groups exhibited a hyperopic shift in refraction. Atropine is known to affect the choroid, inducing thickening as observed in previous studies[33–36]. At baseline, CT was significantly greater in hyperopic children. After treatment, CT increased significantly in myopic children but remained unchanged in hyperopic children. Jiang et al. reported that 1 week of 1% atropine treatment increased CT in both myopic patients and controls, with greater thickening observed in the myopic group[38]. This finding aligns with the more pronounced CT increase we observed in our myopic group. Araki et al. found no significant CT change after atropine in amblyopic eyes with higher hyperopia, whereas the fellow eye showed an increase[39]. Although we also found no significant changes in CT in hyperopic children, the underlying mechanism might be different, given that our patients were not amblyopic (all BCVA < 0.155).

The mechanism of choroidal thickening caused by atropine is still unclear. Zhang et al.[35] proposed the potential involvement of mechanical traction from the ciliary muscle, tension in choroidal nonvascular smooth muscles, and the blockade of related receptors. Modulation of choroidal blood flow by atropine may also contribute

to its mechanism. Choroidal blood flow is reduced in myopic eyes compared with controls[40,41]. Atropine increases choroidal blood flow and inhibits the reduction associated with myopia[42], potentially leading to increased CT. This mechanism may explain the greater change in CT in myopic children. However, choroidal blood flow in hyperopic children after atropine has not been well studied. Therefore, the mechanism of CT changes in children with hyperopia remains to be explored.

Using AS-OCT, we observed changes in the ciliary muscle after short-term atropine treatment. We employed manual measurement of the ciliary muscle's biometry to overcome the limitations of automated segmentation due to low contrast at the posterior ciliary muscle boundary. Manual measurement is a well-established and reliable method used in ciliary muscle studies[27,43–46].

We found no significant between-group differences in anterior ciliary muscle thickness, but the posterior region was thinner in the hyperopia group. AL was positively correlated with posterior ciliary muscle thickness but not with anterior thickness. A similar relationship between CMT and AL has been observed in previous studies[19,27]. However, Bailey et al. also found that CMT1 was weakly correlated with AL[27]. Wagner et al. found that the anterior ciliary muscle of myopic eyes was thinner[44]. Although we observed a trend towards thinner CMT1 in myopic eyes, it was not statistically significant, possibly due to the limited sample size. We also found an association between CMT and CT: thicker posterior ciliary muscle was associated with a thinner choroid. However, this association was no longer significant after adjusting for AL, suggesting that the relationship between choroidal and ciliary muscle thickness is mediated by AL.

Our results are in line with the hypothesis that the choroid is stretched[47]. The anterior area of the ciliary muscle mainly comprises circular and radial fibers, whereas the posterior area mainly
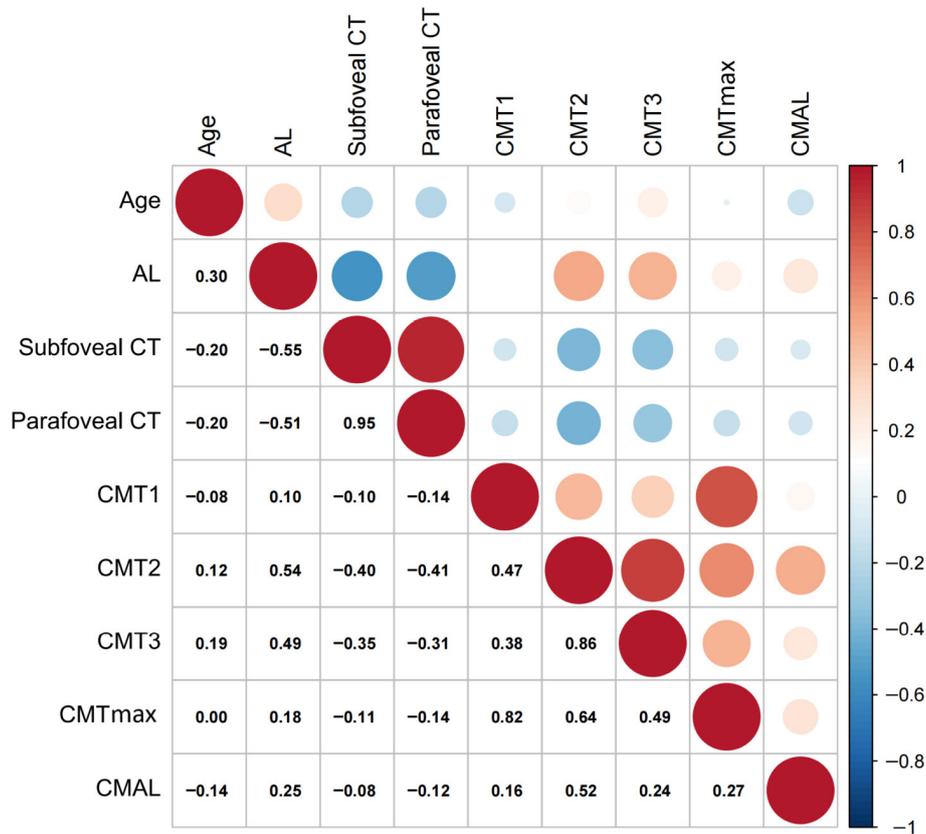
Fig. 4 Heatmap of the correlations among age, baseline anterior segment biometry, baseline choroidal thickness, and baseline ciliary muscle biometry (n = 48 eyes). The number in the grid on the lower left side of the picture is the Pearson correlation coefficient of the two parameters in the vertical and horizontal columns. The colored dots on the upper right-hand side of the picture are the correlation coefficients presented in color. The right side of the picture shows the relationship between color and correlation coefficient. Red dots represent positive correlations, and blue dots represent negative correlations. The size of the dots represents the p-value of the Pearson correlation coefficient. The larger the dot, the more significant the correlation. AL, axial length; CT, choroidal thickness; CMT1, ciliary muscle thickness at 1 mm from the scleral spur; CMT2, ciliary muscle thickness at 2 mm from the scleral spur; CMT3, ciliary muscle thickness at 3 mm from the scleral spur; CMTmax, maximum ciliary muscle thickness; CMAL, tangent length from the ciliary muscle apex to the scleral spur.

consists of longitudinal fibers[8–11]. Thickening of the posterior region appears to be more closely associated with myopia. As the longitudinal fibers originate near the choroid and insert near the limbus, their contraction during accommodation pulls the choroid anteriorly, potentially contributing to choroidal thinning and axial elongation[47]. Additionally, Bailey's theory of ciliary muscle hypertrophy may also contribute to explaining this mechanism[27]. The hypertrophic ciliary muscle might serve as an equatorial growth restriction, leading to myopic axial elongation[48]. Hypertrophic smooth muscle may exhibit impaired contractility, and ciliary muscle hypertrophy is thought to contribute to the characteristic accommodation dysfunction in juvenile myopia[27]. However, the causal relationship between accommodation lag and the onset of myopia is still unclear[49,50]. Further longitudinal studies are needed to elucidate the relationship between ciliary muscle hypertrophy and the development of myopia.

We also investigated the influence of age on the ciliary muscle. The correlation between age and CMT has been demonstrated in previous studies[16,26]. However, we found no correlation between age and any ciliary parameter, likely attributable to the narrow age range of our cohort.

After short-term atropine treatment, we observed outward displacement and thickening of the ciliary muscle's apex. In most studies, the anterior ciliary muscle thickened during accommodation, while the posterior ciliary muscle thinned or did not significantly change[17–23]. If atropine solely induces cycloplegia, anterior ciliary muscle thinning would be expected. Zhou et al. reported a decreased CMTmax after administration of 1% atropine[45], consistent with this expectation. However, the low resolution of the UBM, direct contact, and differences in image analysis may affect the measurement[43]. In another study using phenylephrine, no difference in CMT was observed after administration[51].

Our findings differ from those of Zhou et al. We found thickening throughout the ciliary muscle (in the emmetropic and hyperopic groups) and particularly in the posterior region (all groups), suggesting that atropine may have effects beyond cycloplegia. Potential mechanisms include enhanced unconventional aqueous outflow[52–54] and shared neurovascular regulation between the ciliary muscle and the choroid[35,39,55]. However, the precise mechanisms remain to be determined and require future investigation.

Multiple regression analysis was used to identify predictors of changes in the ciliary muscle's biometry after administration of atropine. We found that a thicker baseline ciliary muscle was associated with less thickening after atropine treatment. However, age, sex, ACD, and CT were not significant predictors. Moreover, baseline CMT1 and CMAL were independently associated with SE. For a given baseline CMT1 value, a lower (more myopic) SE was associated with a smaller change in CMT1. Wagner et al. observed that changes in the ciliary muscle occurred more posteriorly during accommodation in myopic eyes than in emmetropic eyes[23]. We speculate that

although the anterior ciliary muscle's morphology appeared to be normal at baseline in myopic children, its contractility may have been impaired. Furthermore, for a given baseline CMAL value, a higher degree of myopia was associated with greater posterior displacement of the ciliary muscle apex (ΔCMAL), supporting the notion of more posterior changes in myopic ciliary muscle. However, the differences in ΔCMT between groups might also reflect varying degrees of accommodative reduction. Myopic children may have accommodated less to viewing the fixation target prior to atropine compared with hyperopic children.

We applied a refractive index of 1.000[27] to the entire image, resulting in an overestimation of the absolute thickness values. Given the variations in the reported refractive index of human ciliary muscle[56–59], correction methods[18,20,22,27,29], and measurement techniques[18,20,56–58] across studies, a direct quantitative comparison of absolute ciliary muscle parameters between studies is difficult. However, all measurements in this study were obtained using consistent equipment and procedures, ensuring comparability within our dataset. Therefore, we focused on the qualitative results of different studies.

Additionally, manual measurement introduces potential subjectivity by the technician. To mitigate this effect, each patient visit was assigned a unique code unrelated to identifiable information or visit sequence. Another limitation was the relatively small sample sizes, particularly for the myopic ($n = 12$) and hyperopic ($n = 19$) subgroups, limiting the statistical power in group comparisons and potentially increasing the risk of Type II errors (false negatives). Moreover, we assessed only morphological parameters. The lack of functional assessments precluded a quantification of the ciliary muscle–accommodation relationship. Additionally, the short-term atropine regimen used here differs from protocols for long-term myopia control. The effect of atropine on the ciliary muscle needs to be further explored under different conditions. Furthermore, our results are confounded by cycloplegia. To isolate specific atropine effects, comparisons with other cycloplegic agents are needed. Furthermore, all participants were children without refractive correction. Hyperopic children have higher accommodative demands, and the observed changes after atropine treatment might reflect greater release of accommodation in this group, potentially confounding the results.

Conclusions

Before atropine treatment, CMT2 and CMT3 differed significantly among the refractive groups and showed positive correlations with AL. CMT2 was negatively correlated with CT, which is consistent with the choroidal stretching hypothesis. Hyperopic drift was observed after short-term atropine treatment. CT increased significantly in myopic children but remained unchanged in hyperopic children. Contrary to the expected thinning of the anterior ciliary muscle with cycloplegia, the entire ciliary muscle thickened following atropine treatment. Atropine might have other effects on the ciliary muscle in addition to cycloplegia.

Ethical statements

The study was conducted in accordance with the Declaration of Helsinki. The study protocol was approved by the Ethics Committee of Shanghai General Hospital, Shanghai Jiao Tong University (2020KY018), and written informed consent was obtained from the participants and their parents.

Author contributions

The authors confirm their contributions to the paper as follows: study conception and design: Xu Y; data collection: Cui LP, Tang C; analysis and interpretation of results: Xiang ZY; draft manuscript preparation: Xiang ZY, Zou HD. All authors reviewed the results and approved the final version of the manuscript.

Data availability

The datasets generated and analyzed during the current study are not publicly available due to patient confidentiality but are available from the corresponding author upon reasonable request.

Acknowledgments

Conflict of interest

The authors declare that they have no conflict of interest.

Dates

References

1. Gong Q, Janowski M, Luo M, Wei H, Chen B, et al. 2017. Efficacy and adverse effects of atropine in childhood myopia: a meta-analysis. *JAMA Ophthalmology* 135:624–30

2. Papageorgiou E, Asproudis I, Maconachie G, Tsironi EE, Gottlob I. 2019. The treatment of amblyopia: current practice and emerging trends. *Graefe's Archive for Clinical and Experimental Ophthalmology* 257:1061–78

3. Anderson HA, Glasser A, Stuebing KK, Manny RE. 2009. Minus lens stimulated accommodative lag as a function of age. *Optometry and Vision Science* 86:685–94

4. Harrington SC, Stack J, O'Dwyer V. 2019. Risk factors associated with myopia in schoolchildren in Ireland. *British Journal of Ophthalmology* 103:1803–9

5. Singh NK, James RM, Yadav A, Kumar R, Asthana S, et al. 2019. Prevalence of myopia and associated risk factors in schoolchildren in North India. *Optometry and Vision Science* 96:200–5

6. Wang J, Ying GS, Fu X, Zhang R, Meng J, et al. 2020. Prevalence of myopia and vision impairment in school students in Eastern China. *BMC Ophthalmology* 20:2

7. Hughes RPJ, Read SA, Collins MJ, Vincent SJ. 2020. Changes in ocular biometry during short-term accommodation in children. *Ophthalmic & Physiological Optics* 40:584–94

8. Lütjen E. 1966. Histometric studies on the ciliary muscle in primates [Histometrische Untersuchungen über den Ciliarmuskel der Primaten]. *Albrecht Von Graefe's Archive for Clinical and Experimental Ophthalmology* 171:121–33

9. Lütjen-Drecoll E, Tamm E, Kaufman PL. 1988. Age-related loss of morphologic responses to pilocarpine in rhesus monkey ciliary muscle. *Archives of Ophthalmology* 106:1591–98

10. Rohen JW, Kaufman PL, Eichhorn M, Goeckner PA, Bito LZ. 1989. Functional morphology of accommodation in the raccoon. *Experimental Eye Research* 48:523–27

11. Neider MW, Crawford K, Kaufman PL, Bito LZ. 1990. *In vivo* videography of the rhesus monkey accommodative apparatus. Age-related loss of ciliary muscle response to central stimulation. *Archives of Ophthalmology* 108:69–74

12. Croft MA, Kaufman PL, Crawford KS, Neider MW, Glasser A, et al. 1998. Accommodation dynamics in aging rhesus monkeys. *The American Journal of Physiology* 275:R1885–R1897

13. Glasser A, Kaufman PL. 1999. The mechanism of accommodation in primates. *Ophthalmology* 106:863–72

14. Ostrin LA, Glasser A. 2007. Edinger-Westphal and pharmacologically stimulated accommodative refractive changes and lens and ciliary process movements in rhesus monkeys. *Experimental Eye Research* 84:302–13

15. Croft MA, Glasser A, Heatley G, McDonald J, Ebbert T, et al. 2006. Accommodative ciliary body and lens function in rhesus monkeys, I: normal lens, zonule and ciliary process configuration in the iridectomized eye. *Investigative Ophthalmology & Visual Science* 47:1076–86

16. Croft MA, McDonald JP, Katz A, Lin TL, Lütjen-Drecoll E, et al. 2013. Extralenticular and lenticular aspects of accommodation and presbyopia in human versus monkey eyes. *Investigative Ophthalmology & Visual Science* 54:5035–48

17. Lossing LA, Sinnott LT, Kao CY, Richdale K, Bailey MD. 2012. Measuring changes in ciliary muscle thickness with accommodation in young adults. *Optometry and Vision Science* 89:719–26

18. Xie X, Sultan W, Corradetti G, Lee JY, Song A, et al. 2022. Assessing accommodative presbyopic biometric changes of the entire anterior segment using single swept-source OCT image acquisitions. *Eye* 36:119–28

19. Lewis HA, Kao CY, Sinnott LT, Bailey MD. 2012. Changes in ciliary muscle thickness during accommodation in children. *Optometry and Vision Science* 89:727–37

20. Mohamed Farouk M, Naito T, Shinomiya K, Mitamura Y. 2018. Observation of ciliary body changes during accommodation using anterior OCT. *The Journal of Medical Investigation* 65:60–63

21. Richdale K, Bullimore MA, Sinnott LT, Zadnik K. 2016. The effect of age, accommodation, and refractive error on the adult human eye. *Optometry and Vision Science* 93:3–11

22. Chen L, Jin W, Hao X, Li X, Xing Y. 2021. Dynamic changes of scleral spur length in different accommodation stimuli states. *Scientific Reports* 11:18176

23. Wagner S, Schaeffel F, Zrenner E, Straßer T. 2019. Prolonged nearwork affects the ciliary muscle morphology. *Experimental Eye Research* 186:107741

24. Oliveira C, Tello C, Liebmann JM, Ritch R. 2005. Ciliary body thickness increases with increasing axial myopia. *American Journal of Ophthalmology* 140:324–25

25. Fernández-Vigo JI, Shi H, Kudsieh B, Arriola-Villalobos P, De-Pablo Gómez-de-Liaño L, et al. 2020. Ciliary muscle dimensions by swept-source optical coherence tomography and correlation study in a large population. *Acta Ophthalmologica* 98:e487–e494

26. Muftuoglu O, Hosal BM, Zilelioglu G. 2009. Ciliary body thickness in unilateral high axial myopia. *Eye* 23:1176–81

27. Bailey MD, Sinnott LT, Mutti DO. 2008. Ciliary body thickness and refractive error in children. *Investigative Ophthalmology & Visual Science* 49:4353–60

28. Pucker AD, Sinnott LT, Kao CY, Bailey MD. 2013. Region-specific relationships between refractive error and ciliary muscle thickness in children. *Investigative Ophthalmology & Visual Science* 54:4710–16

29. Buckhurst H, Gilmartin B, Cubbidge RP, Nagra M, Logan NS. 2013. Ocular biometric correlates of ciliary muscle thickness in human myopia. *Ophthalmic & Physiological Optics* 33:294–304

30. Kuchem MK, Sinnott LT, Kao CY, Bailey MD. 2013. Ciliary muscle thickness in anisometropia. *Optometry and Vision Science* 90:1312–20

31. Shi J, Zhao J, Zhao F, Naidu R, Zhou X. 2020. Ciliary muscle morphology and accommodative lag in hyperopic anisometropic children. *International Ophthalmology* 40:917–24

32. Wu PC, Chuang MN, Choi J, Chen H, Wu G, et al. 2019. Update in myopia and treatment strategy of atropine use in myopia control. *Eye* 33:3–13

33. Ye L, Li S, Shi Y, Yin Y, He J, et al. 2021. Comparisons of atropine versus cyclopentolate cycloplegia in myopic children. *Clinical & Experimental Optometry* 104:143–50

34. Nickla DL, Zhu X, Wallman J. 2013. Effects of muscarinic agents on chick choroids in intact eyes and eyecups: evidence for a muscarinic mechanism in choroidal thinning. *Ophthalmic & Physiological Optics* 33:245–56

35. Zhang Z, Zhou Y, Xie Z, Chen T, Gu Y, et al. 2016. The effect of topical atropine on the choroidal thickness of healthy children. *Scientific Reports* 6:34936

36. Sander BP, Collins MJ, Read SA. 2019. Short-term effect of low-dose atropine and hyperopic defocus on choroidal thickness and axial length in young myopic adults. *Journal of Ophthalmology* 2019:4782536

37. Zhou Y, Zhu Y, Huang XB, Xiong YJ, Guo YL, et al. 2023. Changes of choroidal thickness in children after short-term application of 1% atropine gel. *Ophthalmic Research* 66:421–30

38. Jiang Y, Zhang Z, Wu Z, Sun S, Fu Y, et al. 2021. Change and recovery of choroid thickness after short-term application of 1% atropine gel and its influencing factors in 6-7-year-old children. *Current Eye Research* 46:1171–77

39. Araki S, Miki A, Goto K, Fujiwara A, Yamashita T, et al. 2023. Changes in choroidal thickness and structure induced by 1% atropine instillation in children with hyperopic anisometropic amblyopia. *Journal of Pediatric Ophthalmology and Strabismus* 60:39–45

40. Yang YS, Koh JW. 2015. Choroidal blood flow change in eyes with high myopia. *Korean Journal of Ophthalmology* 29:309–14

41. Liu F, Niu L, Guo J, Jian W, Shang J, et al. 2023. Quantitative evaluation of retinal and choroidal vascularity and retrobulbar blood flow in patients with myopic anisometropia by CDI and OCTA. *British Journal of Ophthalmology* 107:1172–77

42. Zhou X, Zhang S, Zhang G, Chen Y, Lei Y, et al. 2020. Increased choroidal blood perfusion can inhibit form deprivation myopia in guinea pigs. *Investigative Ophthalmology & Visual Science* 61:25

43. Chang YC, Liu K, Cabot F, Yoo SH, Ruggeri M, et al. 2018. Variability of manual ciliary muscle segmentation in optical coherence tomography images. *Biomedical Optics Express* 9:791–800

44. Wagner S, Zrenner E, Strasser T. 2019. Emmetropes and myopes differ little in their accommodation dynamics but strongly in their ciliary muscle morphology. *Vision Research* 163:42–51

45. Zhou Y, Huang XB, Cai Q, Li JJ, Xiong YJ, et al. 2020. Comparative study of the effects of 1% atropine on the anterior segment. *Journal of Ophthalmology* 2020:5125243

46. Bailey MD. 2011. How should we measure the ciliary muscle? *Investigative Ophthalmology & Visual Science* 52:1817–18

47. Van Alphen GWHM. 1986. Choroidal stress and emmetropization. *Vision Research* 26:723–34

48. Mutti DO, Hayes JR, Mitchell GL, Jones LA, Moeschberger ML, et al. 2007. Refractive error, axial length, and relative peripheral refractive error before and after the onset of myopia. *Investigative Ophthalmology & Visual Science* 48:2510–19

49. Gwiazda J, Thorn F, Held R. 2005. Accommodation, accommodative convergence, and response AC/A ratios before and at the onset of myopia in children. *Optom Vis Sci* 82:273–8

50. Mutti DO, Mitchell GL, Hayes JR, Jones LA, Moeschberger ML, et al. 2006. Accommodative lag before and after the onset of myopia. *Investigative Ophthalmology & Visual Science* 47:837–46

51. Richdale K, Bailey MD, Sinnott LT, Kao CY, Zadnik K, et al. 2012. The effect of phenylephrine on the ciliary muscle and accommodation. *Optometry and Vision Science* 89:1507−11

52. Bill A. 1967. Effects of atropine and pilocarpine on aqueous humour dynamics in cynomolgus monkeys (*Macaca irus*). *Experimental Eye Research* 6:120−25

53. Bill A. 1969. Effects of atropine on aqueous humor dynamics in the vervet monkey (*Cercopithecus ethiops*). *Experimental Eye Research* 8:284−91

54. Bill A, Phillips CI. 1971. Uveoscleral drainage of aqueous humour in human eyes. *Experimental Eye Research* 12:275−81

55. McDougal DH, Gamlin PD. 2015. Autonomic control of the eye. *Comprehensive Physiology* 5:439−73

56. Wagner S, Zrenner E, Strasser T. 2018. Ciliary muscle thickness profiles derived from optical coherence tomography images. *Biomedical Optics Express* 9:5100−14

57. Sheppard AL, Davies LN. 2010. *In vivo* analysis of ciliary muscle morphologic changes with accommodation and axial ametropia. *Investigative Ophthalmology & Visual Science* 51:6882−89

58. Sheppard AL, Davies LN. 2011. The effect of ageing on *in vivo* human ciliary muscle morphology and contractility. *Investigative Ophthalmology & Visual Science* 52:1809−16

59. Kao CY, Richdale K, Sinnott LT, Grillott LE, Bailey MD. 2011. Semiautomatic extraction algorithm for images of the ciliary muscle. *Optometry and Vision Science* 88:275−89